Diabetes, Metabolic Syndrome and Obesity

Dovepress
Taylor & Francis Group

Open Access Full Text Article

ORIGINAL RESEARCH

Proteomic Analysis of the Effects of Shenzhu Tiaopi Granules on Model Rats with Type 2 Diabetes Mellitus

Jin-Dong Zhao[1–3], Zhao-Hui Fang[1–3]

[1]Department of Endocrinology Two, the First Affiliated Hospital of Anhui University of Chinese Medicine, Hefei, Anhui Province, 230031, People's Republic of China; [2]Center for Xin'an Medicine and Modernization of Traditional Chinese Medicine of IHM, the First Affiliated Hospital of Anhui University of Chinese Medicine, Hefei, Anhui Province, 230012, People's Republic of China; [3]Diabetes Institute, Anhui Academy Chinese Medicine, Hefei, 230012, People's Republic of China

Correspondence: Zhao-Hui Fang, Department of Endocrinology Two, the First Affiliated Hospital of Anhui University of Chinese Medicine, 117 Meishan Road, Hefei, Anhui Province, 230031, People's Republic of China, Email fangzhaohui1111@163.com

Diabetes, Metabolic Syndrome and Obesity downloaded from https://www.dovepress.com/
For personal use only.

Background: Shenzhu Tiaopi granule (STG) has antidiabetic functions. Data-independent acquisition proteomic technology is an integral part of systems biology. Herein, proteomics was used to analyse the effects of STG on type 2 diabetes mellitus (T2DM) and the mechanism by which STG normalizes glucose metabolism.

Methods: Goto-Kakizaki (GK) T2DM model (Mod) rats, aged 15–16 weeks and with a fasting blood glucose (FBG) level of ≥11.1 mmol/L, were treated with metformin or STG for 12 weeks. Wistar rats aged 15–16 weeks were included in the control (Con) group. Body weight, FBG, total cholesterol (TC), total triglyceride (TG) levels and low-density lipoprotein (LDL-C) levels were measured, and pathological observation, Western blot analysis and data-independent acquisition proteomics of the liver were performed.

Results: Significant differences in FBG, TC, TG, LDL-C ($p < 0.01$) and pathological liver morphology were observed between the Mod group and Con group, whereas both metformin and STG normalized the glucose and lipid metabolism indicators ($p < 0.05$ or $p < 0.01$). In total, 5856 proteins were identified via proteomic analysis, 97 of which were significantly differentially expressed in the liver and affected fatty acid metabolism, unsaturated fatty acid biosynthesis, the peroxisome proliferator-activated receptor (PPAR) signalling pathway, pyruvate metabolism, and terpenoid backbone biosynthesis. Screening identified 10 target proteins, including perilipin-2 (Plin2), pyruvate dehydrogenase kinase 4, farnesyl diphosphate synthase (Fdps) and farnesyl-diphosphate farnesyltransferase 1. Among these proteins, the key proteins were Plin2 and Fdps, which were found to be associated with the PPAR signalling pathway and terpenoid backbone biosynthesis via relationship networks. Plin2 and Fdps are closely related to hyperglycaemia. STG can downregulate Plin2 and upregulate Fdps ($p < 0.01$).

Conclusion: STG ameliorated hyperglycaemia by significantly altering the expression of different proteins, especially Fdps and Plin2, in the livers of GK rats. These findings may reveal the potential of traditional Chinese medicine for treating T2DM.

Keywords: type 2 diabetes mellitus, improving hyperglycaemia, proteomics, Fdps, Plin2, Shenzhu Tiaopi granule

Introduction

Type 2 diabetes mellitus (T2DM) is a very common metabolic disease characterised by hyperglycaemia that can lead to many serious complications. Therefore, T2DM is considered a major health concern.[1,2] The liver plays an important role in maintaining glucose homeostasis in the body, particularly through hepatic gluconeogenesis and glycogen synthesis.[3] Metformin (Met) is widely used to treat T2DM by lowering blood glucose through the inhibition of glucose output from the liver. The main adverse effects associated with Met use are gastrointestinal reactions and vitamin B12 deficiency.[4]

Compared with metabolomics and genomics, proteomics can better describe the mechanism of protein action in vivo and reveal new therapeutic targets.[5,6] Data-independent acquisition (DIA) proteomics has been extensively developed for identification of novel differentially expressed targets.[7] DIA proteomics achieves precise and highly reproducible

Received: 25 August 2024
Accepted: 22 January 2025
Published: 25 February 2025

© 2025 Zhao and Fang. This work is published and licensed by Dove Medical Press Limited. The full terms of this license are available at https://www.dovepress.com/terms.php and incorporate the Creative Commons Attribution – Non Commercial (unported, v3.0) License (http://creativecommons.org/licenses/by-nc/3.0/). By accessing the work you hereby accept the Terms. Non-commercial uses of the work are permitted without any further permission from Dove Medical Press Limited, provided the work is properly attributed. For permission for commercial use of this work, please see paragraphs 4.2 and 5 of our Terms (https://www.dovepress.com/terms.php).

quantification of large amounts of proteins in each sample, including low-abundance protein information. Reliable therapeutic protein biomarkers can be found via proteomic analysis of T2DM samples.[8] The GCKR, HLA-DRA, RAB1A, ARG1, and HHIP proteins and other plasma proteins are associated with T2DM according to proteome-wide Mendelian randomization.[9] A study revealed that extracellular vesicles in the liver proteomic and phosphoproteomic signatures of T2DM patients may underlie the development of T2DM.[10] In recent years, researchers have applied proteomics to explore the mechanism of action of traditional Chinese medicine (TCM) in treating diseases, which is a method used in the study of the pharmacological mechanisms of TCM.[11,12] The effects of TCM in T2DM patients can be identified by proteomic differences.[13] With respect to proteomic technology, Tianqi Jiangtang Capsule can be used to treat T2DM via regulation of serum protein profiles.[14] Mulberry leaf treatment reversed the changes in 19 differentially expressed proteins in rats with T2DM according to proteomic analysis of skeletal muscle.[15]

Previous studies have suggested that TCM could be effective for treating T2DM. Goto-Kakizaki (GK) rats are a spontaneous T2DM research model. When these rats are 15–16 weeks old, they exhibit hyperglycaemia.[16] This model shows less mortality than does the chemical-induced diabetes model. Moreover, the blood glucose level can be used to diagnose diabetes without being very high. Shenzhu Tiaopi granule (STG) is an herbal compound formula that has been used to treat pre-T2DM and T2DM and can lower blood glucose, alleviate thirst, and relieve fatigue and has other effects.[17–19] However, the mechanism by which STG regulates blood glucose is not clear. DIA proteomics has the advantage of being more precise than traditional proteomics. In this study, we conducted DIA proteomic studies to further determine the impact of STG on liver glucose metabolism in a T2DM rat model. Furthermore, glycolipid metabolism indicators were used to investigate the effects. This study may help elucidate the mechanism by which STG alleviates T2DM, which may lead to the development of potential therapeutic biomarkers of TCM against T2DM.

Materials and Methods

Animals and Treatment

All animal procedures were performed in accordance with the Guidelines for the Care and Use of Laboratory Animals and were approved by the Animal Ethics Committee of Anhui University of Chinese Medicine (AHUCM-rats-2021133). GK rats (n = 70, male) aged 5–6 weeks were obtained from Changzhou Cavens Model Animal Co., Ltd. (China; certificate no. 202145537). Wistar rats (n = 10, male) aged 5–6 weeks were obtained from SiBeifu (Beijing) Biotechnology Co., Ltd. (China; certificate no. 110324210106755915). All the animals were housed on a 12-hour dark–light cycle at 25 ± 2 °C and were allowed to eat and drink freely. The animals were acclimated to standard laboratory conditions for 10 weeks before being assigned to an experimental group. GK rats (n = 32) with fasting blood glucose (FBG) levels ≥11.1 mmol/L were used. The GK rats were then randomly divided into a model (Mod) group, a Met group, and a STG group (n = 8 per group). The Wistar rats composed the control (Con) group (n = 8) (Figure 1). All the rats were fed a standard chow diet. The Met group was orally administered a Met aqueous solution at a dosage of 150 mg/kg/d (Shanghai MACKLIN Biochemical Technology Co., Ltd, China). The STG group was orally administered STG extract (The First Affiliated Hospital of Anhui University of Chinese Medicine, China) at a dosage of 21 g/kg/d.[20] After 12 weeks of intervening, the rats were fasted, and

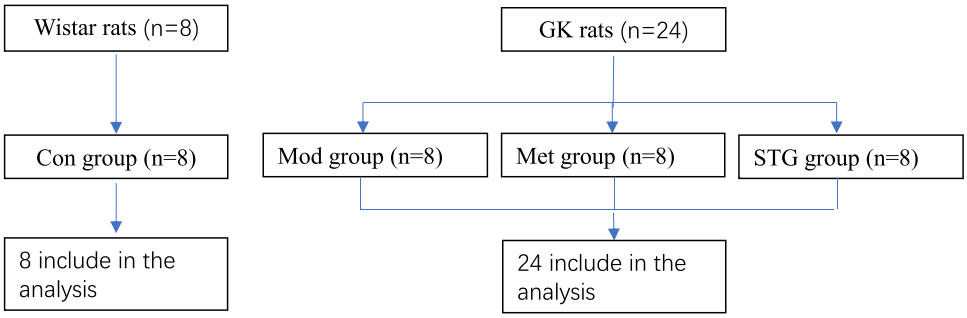

Figure 1 Animal flow chart.
Abbreviations: GK, Goto-Kakizaki; Con, control; Mod, model; Met, metformin; STG, Shenzhu Tiaopi granule.

their body weights were determined with a scale. FBG levels were measured in blood samples acquired via the tail vein via a glucose metre (ACCUCHEK Performa, Roche, Basel, Switzerland). All animals were sacrificed via 3% sodium pentobarbital anaesthesia. Blood was collected in a tube and centrifuged (3000 × g, 15 minutes) to obtain serum, which was stored at −80 °C. Liver tissues were dissected and weighed. The liver index was calculated as the liver weight/body weight. Partial livers from the same anatomical site were fixed with 4% neutral formaldehyde fixative (Beijing Labgic Technology Co., Ltd.), while the remaining tissues were stored at –80 °C.

Preparation of STG

STG consisted of *Codonopsis Radix* (Bozhou Huqiao Pharmaceutical Co., Ltd, China)., *Atractylodis Macrocephalae Rhizoma* (Anhui Mengshi Traditional Chinese Medicine Pieces Co., Ltd, China)., *Pinelliae Rhizoma* (Anhui Puren Traditional Chinese Medicine Pieces Co., Ltd, China)., *Poria* (Anhui Puren Traditional Chinese Medicine Pieces Co., Ltd)., *Aurantii Fructus* (Anhui Puren Traditional Chinese Medicine Pieces Co., Ltd, China)., *Coptidis Rhizoma* (Anhui Xiehecheng Pharmaceutical Co., Ltd, China)., *Dioscoreae Rhizoma* (Bozhou Huqiao Pharmaceutical Co., Ltd, China)., *Bupleuri Radix* (Anhui Xiehecheng Pharmaceutical Co., Ltd, China)., *Gypsum Fibrosum* (Bozhou Huqiao Pharmaceutical Co., Ltd, China)., *Lophatherum gracile* (Anhui Puren Traditional Chinese Medicine Pieces Co., Ltd, China)., and *Ophiopogonis Radix* (Anhui Xiehe Cheng Pharmaceutical Co., Ltd, China). The ratio of this dose was 10:10:4:5:5:2:10:4:5:10:5. A total of 210 g of STG was weighed and soaked in 2100 mL of water in a decoction container for 30 minutes. The STG was boiled over high heat and then simmered over low heat for 30 minutes. The mixture was filtered through a strainer, and the medicinal mixture was collected. Then, 2100 mL of water was added again, and the same boiling method was used as before. The two medicinal solutions were combined to obtain the STG medicinal mixture. The obtained extraction mixture was concentrated to 50 mL, with a crude concentration of 4.2 g/mL, sealed, and stored at 4 °C.

Liquid Chromatography–Mass Spectrometry (LC–MS) Detection and Metabolite Identification

Fifty microlitres of the STG extraction mixture was transferred into a centrifuge tube, 400 μL of methanol:acetonitrile (1:1) was added, and the mixture was extracted by ultrasonication at 5 °C for 30 minutes. The extraction mixture was left to stand at –20 °C for 30 min and then centrifuged at 13,000 × g for 15 min at 4 °C, after which the supernatant was removed, dried with nitrogen, and dissolved in 100 μL of acetonitrile:water (1:1). The mixture was vortexed and mixed for 30s, after which it was extracted via ultrasonication at 5 °C for 5 minutes. The mixture was subsequently centrifuged at 13,000 × g for 10 minutes at 4 °C, after which the supernatant was transferred to an injection vial with an inner tube for analysis.

The instrument platform for this LC–MS analysis was ultrahigh-performance liquid chromatography–tandem Fourier transform mass spectrometry coupled with ultrahigh-performance liquid chromatography (UHPLC), and the Q Exactive system from Thermo Fisher Scientific (USA) was used. The chromatographic column used was an ACQUITY UPLCBEHC18 (100 mm × 2.1 mm i.d., 1.7 μm). Mobile phase A was 2% acetonitrile in water (containing 0.1% formic acid), mobile phase B was acetonitrile (containing 0.1% formic acid), the injection volume was 3 μL, and the column temperature was 40 °C. The sample was ionized by an electric spray, and the mass spectrum signals were collected in positive and negative ion scanning modes. The quality scanning range was 70–1050 m/z, the heating temperature was 450 °C, the negative ion source voltage was –3000 V, the positive ion source voltage was 3500 V, the cyclic collision energy was 20–40–60 eV, the sheath gas flow rate was 50 arb, and the auxiliary gas flow rate was 13 arb. Positive and negative ion chromatograms were subsequently obtained.

All ion fragment information obtained from mass spectrometric analysis was compared with that of MJBIOTCM (China) to obtain annotation information for the metabolites.

Biochemical Assays and Liver Histological Analysis

The serum total cholesterol (TC), total triglyceride (TG) and low-density lipoprotein (LDL-C) levels were determined via a fully automatic biochemical analyser (Shenzhen Rayto Life Sciences Corporation, China). The reagents used were compatible.

For pathomorphological analysis, the liver was dehydrated in alcohol and cleared with xylene. The samples were subsequently embedded in paraffin, deparaffinized, subjected to haematoxylin–eosin (HE) staining, and finally photographed via light microscopy (Nikon Corporation, Japan) at 200× magnification.

Liver Sample DIA Analysis

Protein Extraction

A total of 12 liver samples were collected from the four groups (3 samples per group). An appropriate amount of liver tissue was weighed and transferred to a 2 mL centrifuge tube, two 5 mm magnetic beads were added, and an appropriate amount of protein lysis solution containing sodium dodecyl sulphate (SDS) and a 1× cocktail with a final concentration of ethylene diamine tetraacetic acid was added. An automatic grinder was used to break and decompose the mixture before it was centrifuged at 25,000 × g and 4 °C for 15 minutes. Next, the supernatant was treated with dithiothreitol at a final concentration of 10 mm and incubated in a water bath at 37 °C for 30 minutes. An iodoacetamide solution with a final concentration of 55 mm was added, and the mixture was left in a dark room for 45 minutes. A total of 5 times the volume of precooled acetone was added next, and the mixture was placed in a –20 °C refrigerator for 2 hours. The mixture was then centrifuged at 25,000 × g and 4 °C for 15 minutes, after which the supernatant was discarded. After precipitation, an appropriate amount of SDS-free protein lysis solution was added, and an automatic grinder was used to promote protein dissolution. The mixture was subsequently centrifuged at 25,000 × g and 4 °C for 15 minutes to obtain the supernatant, which was the protein mixture used for proteomic analysis.[21] Data-independent acquisition protein quantification was performed by BGI (China).

Protein Enrichment Analysis and Digestion

A solid-phase extraction (SPE) C18 column was activated with 1 mL of methanol at a rate of 3 drops/second. Then, 1 mL of 0.1% formic acid solution was added to the SPE C18 column. The diluted serum/plasma protein mixtures were loaded onto and passed through an SPE C18 column at a rate of 1 drop/second. If the volume of the mixture was greater than 1 mL, the operation was repeated 2–3 times. Then, 3 mL of 0.1% formic acid solution was used to wash the nonspecifically bound proteins from the column. The enriched proteins were eluted with 800 μL of 75% acetonitrile at a rate of 0.5 drops/second. The eluate was frozen and dried for further treatment. Next, trypsin was added to the protein mixture at a ratio of 1:20 (w/w) for enzyme and protein analysis, and the mixture was incubated for 14 hours at 37 °C.

DIA Analysis by LC–MS

An Ultimate 3000 nanoLC coupled with a Q Exactive HF mass spectrometer (Thermo Fisher Scientific,USA) was used for LC–MS analysis.[22] The sample was first enriched in the trap column and desalted and then entered a self-packed tandem C18 column (75 μm inner diameter, 1.8 μm particle size, and 25 cm in length) and separated with the following gradient operated at a flow rate of 300 nL/min: 0 minutes, 2% mobile phase B (100% acetonitrile, 0.1% formic acid); 0~45 minutes, mobile phase B linearly increased from 2% to 22%; 45~50 minutes, mobile phase B increased from 25% to 35%; 50~55 minutes, mobile phase B increased from 35% to 80%; and 55~60 minutes, 80% mobile phase B. The end of the nano-LC column was directly connected to the mass spectrometer for MS detection.

The peptides separated by liquid chromatography were ionized by a nanoelectrospray ionization source and then passed to a tandem mass spectrometer for detection in data-dependent acquisition mode. The main parameters were a source voltage of 1.6 kV and a mobility range of 0.6–1.60 $V \cdot S/cm^2$, with a mass spectrometry 1 scanning range of 302–1,077 m/z. A total of 32 windows were used for continuous window fragmentation and data collection. The fragmentation mode was collision-induced dissociation, the fragmentation energy was 10 eV, and the mass width of each window was 25. Each DIA scan cycle lasted 3.3 seconds.

Western Blot Analysis

Liver tissues were homogenized in radioimmunoprecipitation assay lysis buffer and centrifuged at 12,000 × g for 10 min. Total liver proteins were separated by SDS–polyacrylamide gel electrophoresis and transferred onto polyvinylidene fluoride membranes. The membranes were blocked with 5% Tris-buffered saline with Tween and incubated with primary

antibodies overnight at 4 °C. The membranes were washed and incubated for 1 h with secondary antibodies at room temperature. Antibodies targeting Pin2 (ab108323, Abcam), Fdps (ab153805, Abcam), and β-actin (gb11001, Servicebio) were used as loading and comparative controls. The immunoreactive bands were visualized via a chemiluminescence reagent (Wuhan Servicebio Technology Co., Ltd, China). The quantification of the blot results was performed via ImageJ software.

Data and Statistical Analyses

The DIA data were analysed via iRT peptides for retention time calibration. Then, on the basis of the target-decoy model applicable to SWATH-MS, a false-positive control was analysed, with a false discovery rate of 1%, indicating reliable quantitative results.[23] MSstats was used to statistically evaluate differences in protein expression among different samples.[24] Then, screening of the differentially expressed proteins was performed, with the criteria of a fold change >1 or <−1 and a p value < 0.05 indicating a significant difference. OriginPro 2017 was used to perform principal component analysis. Clustering heatmaps were created via Euclidean distance and systematic hierarchical clustering methods. The online Panther database was used to classify the biological functions of the identified proteins. Gene Ontology (GO) enrichment and Kyoto Encyclopedia of Genes and Genomes (KEGG) pathway analyses of the significantly differentially expressed proteins were performed via the nonredundant protein sequence database, GO database, and KEGG database with the analysis platform BGI (China).

The data were analysed via t tests, least significant difference or Tamhane's T2 one-way analysis of variance (ANOVA) tests and nonparametric Kruskal–Wallis 1-way ANOVA tests, and Pearson correlation analysis was performed via IBM SPSS statistics for Windows, version 23 (IBM Corp., USA), and GraphPad Prism 5.0 (GraphPad Software Inc, USA). Values of $p < 0.05$ were considered to indicate a significant difference.

Results

Chemical Profiles of STG

The total negative and positive ion chromatographs of STG are shown in Figure 2A and B. A total of 460 compounds were characterized: 181 phenylpropanoids and polyketides, 10 alkaloids and derivatives, 30 benzenoids, 13 lignans, neolignans and related compounds, 80 lipids and lipid-like molecules, 8 nucleosides, nucleotides, and analogues, 16 organic acids and derivatives, 29 organic oxygen compounds, 35 organoheterocyclic compounds, and 58 other types of compounds. Furthermore, the marker components in STG, including berberine, atractylenolide III, caffeic acid, hesperetin, protocatechuic aldehyde, scopolin, naringin, baicalein, atractyloside A and ferulic acid, may be closely related to hypoglycaemia.

Baseline Information and Liver Histological Analysis

Compared with those in the Con group, the weights in the Mod group were significantly lower ($p < 0.01$). However, there was no significant improvement in weight in the Met group or the STG group. The levels of FBG, TC, TG and LDL-C were significantly greater in the Mod group than in the Con group ($p < 0.01$). Moreover, the FBG, TC, TG and LDL-C levels in the Met and STG groups were significantly lower ($p < 0.01$). The liver indices were significantly greater in the Mod group than in the Con group, and compared with those in the Mod group, the liver indices in the Met and STG groups were significantly lower ($p < 0.05$ or $p < 0.01$) (Table 1).

The liver cells in the Con group were round, plump, and arranged radially. Compared with the Con group, the Mod group presented extensive cellular oedema, severe balloon-like degeneration, cytoplasmic laxity and light staining, widespread fatty degeneration in liver cells, small circular vacuoles in the cytoplasm, and no obvious necrosis or inflammatory cell infiltration. Compared with the Mod group, the Met and STG groups presented improvements in cellular oedema, cytoplasmic laxity, cellular fatty degeneration, and the number of cup-shaped cells (Figure 3).

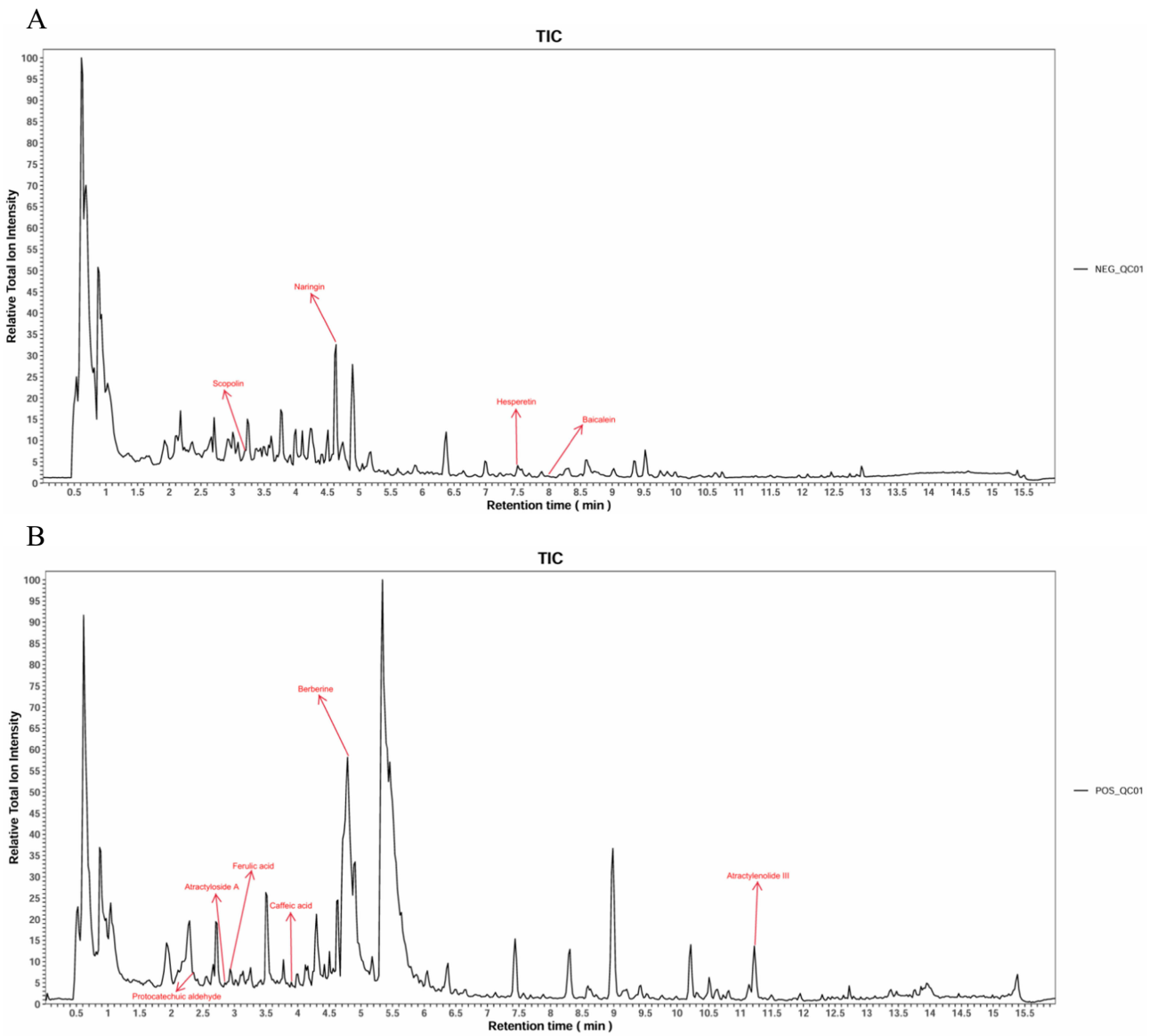

Figure 2 Marker components in STG determined by UHPLC.
Notes: (**A**) Marker components with negative ions in STG according to UHPLC. (**B**) Marker components with positive ions in STG according to UHPLC.
Abbreviations: STG, Shenzhu Tiaopi granule; UHPLC, ultrahigh-performance liquid chromatography; TIC, total ion chromatography; NEG, negative; POS, positive; QC, quality control.

Quantitative Changes in the Liver Proteome

In total, 5856 proteins were identified in the livers from the four different groups. Principal component analysis was performed, as shown in Figure 4A, and all the groups were well separated. In total, 111 proteins (44 increased, 67 decreased) were considered differentially expressed between the Mod and Con groups (Figure 4B and C), 96 proteins (48 increased, 48 decreased) between the Met and Mod groups (Figure 4B and D), 79 proteins (53 increased, 26 decreased) between the STG and Mod groups (Figure 4B and E), and 66 proteins (54 increased, 12 decreased) between the STG and Mod groups (Figure 4B and F). A total of 97 proteins were considered significantly differentially expressed ($p<0.05$) (Figure 4C–F). Moreover, the core common differentially expressed protein was perilipin-2 (Plin2) (Figure 4B).

Table 1 Baseline Information for the Four Groups

Characteristic	Con	Mod	Met	STG
Body weight (g)	511.37±44.06	413.62±20.14**	422.25±24.27	439.75±21.12
Liver index (%)	2.19±0.19	3.88±0.47**	2.64±0.33$^{\#}$	2.33±0.22$^{\#\#}$
FBG (mmol/L)	6.18±0.82	19.56±6.24**	5.86±1.03$^{\#\#}$	8.75±3.14$^{\#\#}$
TG (mmol/L)	0.60±0.24	1.72±0.56**	1.02±0.42	0.73±0.2$^{\#\#}$
TC (mmol/L)	1.61±0.49	2.9±0.71**	1.76±0.21$^{\#\#}$	1.57±0.28$^{\#\#}$
LDL-C (mmol/L)	0.58±0.19	1.25±0.44**	0.50±0.08$^{\#\#}$	0.57±0.11$^{\#\#}$

Notes: Compared with the Con group, **p<0.01. Compared with the Mod group, $^{\#}$p<0.05; $^{\#\#}$p<0.01.
Abbreviations: FBG, fasting blood glucose; TC, total cholesterol; TG, total triglyceride; LDL-C, low-density lipoprotein; Con, control; Mod, model; Met, metformin; STG, Shenzhu Tiaopi granule.

Analysis of Differentially Enriched Proteins

The Mod group revealed significantly upregulated and downregulated proteins than the Con group. Compared with that in the Mod group, protein expression changed significantly after the administration of Met and STG (Figure 5). For example, Plin2 protein expression was upregulated in the Mod group but downregulated in the Met and STG groups. Moreover, the protein expression of fragile X mental retardation (Fmr1), farnesyl diphosphate synthase (Fdps), farnesyl-diphosphate farnesyltransferase 1 (Fdft1) and pyruvate dehydrogenase kinase 4 (Pdk4) decreased in the Mod group but increased in the Met and STG groups.

Liver Proteomic Analysis

As shown in Figure 6A–C, classification based on biological processes revealed that these proteins were related mainly to biological regulation (34.33%), cellular processes (25.67%), metabolic processes (8.98%), and localization (6.42%). The cellular component categories cells, cell parts, organelles and membranes accounted for more than 80% of the

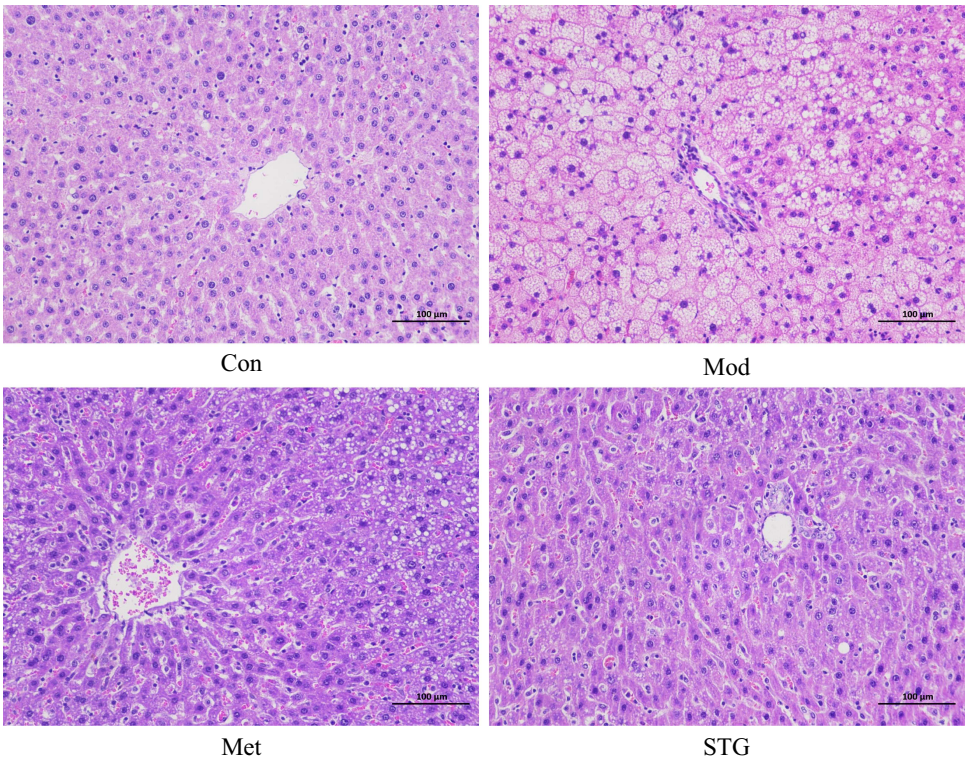

Figure 3 Comparison of HE-stained images of rat liver tissues (200×).
Abbreviations: HE, haematoxylin–eosin;Con, control; Mod, model; Met, metformin; STG, Shenzhu Tiaopi granule.

https://doi.org/10.2147/DMSO.S493036

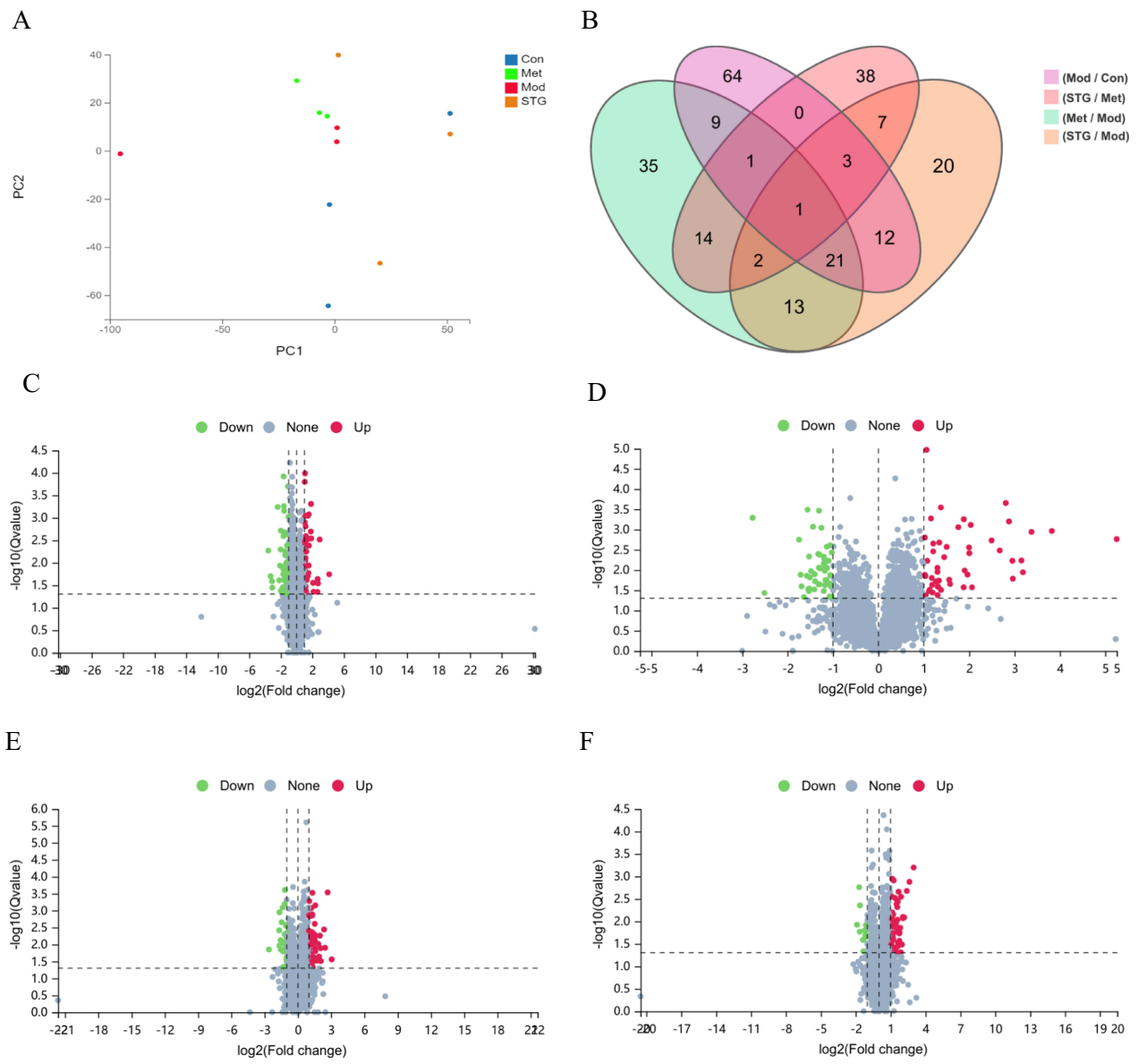

Figure 4 Differences in protein abundance among the four groups.

Notes: (**A**) Principal component analysis of all proteins. (**B**) Venn diagram of significantly differentially expressed proteins. (**C**) Volcano plot of the Mod and Con groups. (**D**) Volcano plot of the Met and Mod groups. (**E**) Volcano plot of the STG and Mod groups. (**F**) Volcano plot of the STG and Met groups. Red represents upregulation, green represents downregulation, and grey represents no significant difference.

Abbreviations: Con, control; Mod, model; Met, metformin; STG, Shenzhu Tiaopi granule; PC1, principal component 1; PC2, principal component 2.

differentially expressed proteins. In terms of molecular function, the differentially expressed proteins were associated mainly with catalytic activity (35.48%) and binding (54.78%).

The differentially expressed proteins in the four groups were involved in 35 metabolic pathways. Compared with the Mod and Con groups, the Met and STG groups showed regulation of multiple pathways. These pathways included fatty acid metabolism, unsaturated fatty acid biosynthesis, the peroxisome proliferator-activated receptor (PPAR) signalling pathway, pyruvate metabolism, terpenoid backbone biosynthesis, steroid hormone biosynthesis and steroid biosynthesis. Among them, the differences in the PPAR signalling pathway were the most significant (Figure 7).

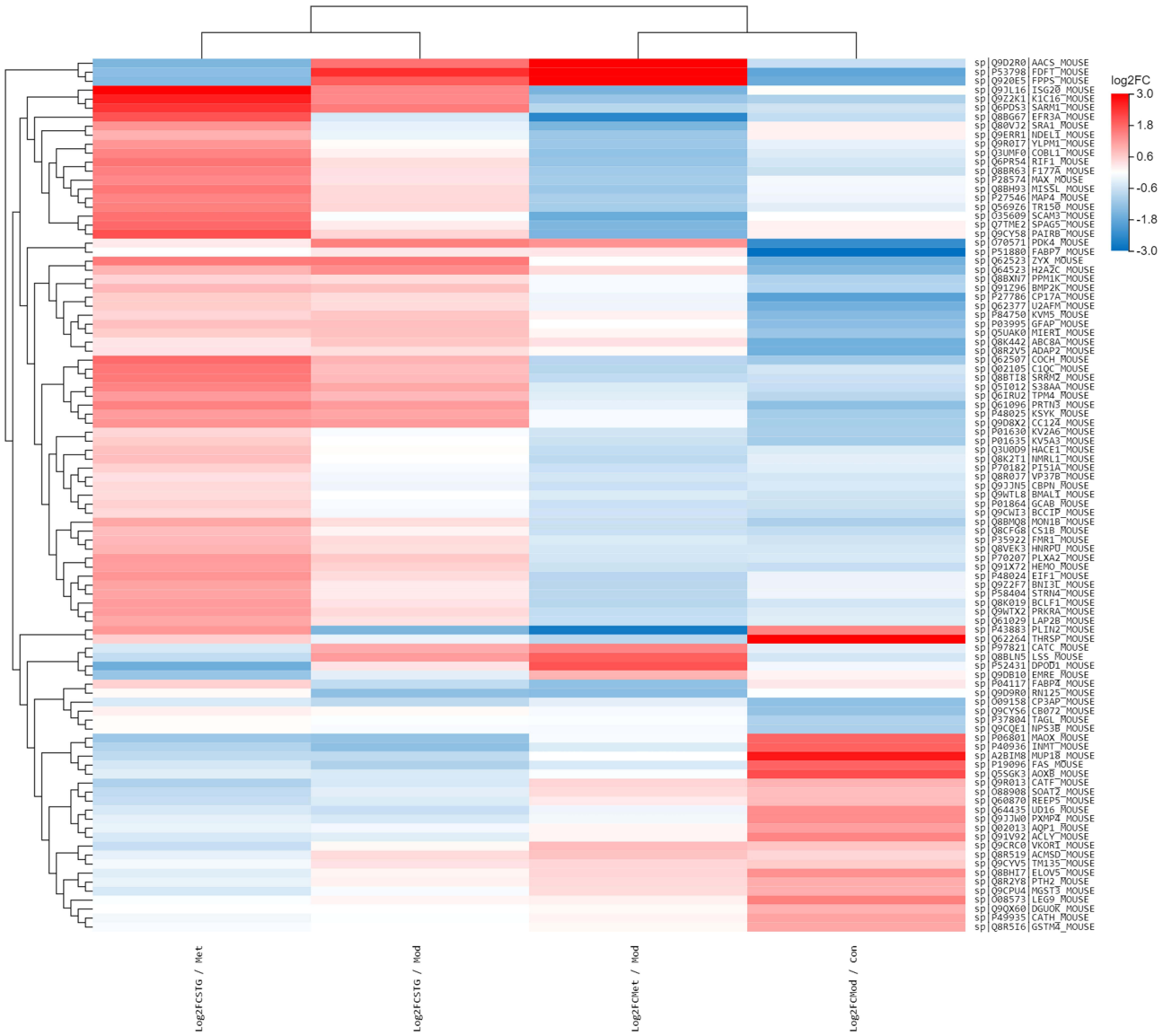

Figure 5 Heatmap of differentially expressed proteins.
Notes: Red represents upregulated proteins, and blue represents downregulated proteins.
Abbreviations: Con, control; Mod, model; Met, metformin; STG, Shenzhu Tiaopi granule.

Screening of the Target Proteins

The differentially expressed proteins were imported into the String 12.0 database, "Rattus norvegicus" was selected as the research species, an average value greater than the degree value was used as the screening criterion, and a confidence level >0.4 was set to construct the differentially expressed protein–protein interaction (PPI) networks (Figure 8A). The network topology characteristics of the PPIs were analysed via Network Analyser with Cytoscape software. On the basis of the DMNC algorithm in the CytoHubba plugin, 10 target proteins, including Plin2, Pdk4, Fdps and Fdft1, were identified by screening (Figure 8B). Figure 8C shows the network of relationships between the differentially expressed proteins and related KEGG pathways, which includes 28 proteins and 10 signalling pathways. Moreover, Plin2 is an important gene in the PPAR signalling pathway. Fdps is an important gene in terpenoid backbone biosynthesis. Among them, 14 proteins were upregulated, and 14 proteins were downregulated in these signalling pathways.

https://doi.org/10.2147/DMSO.S493036

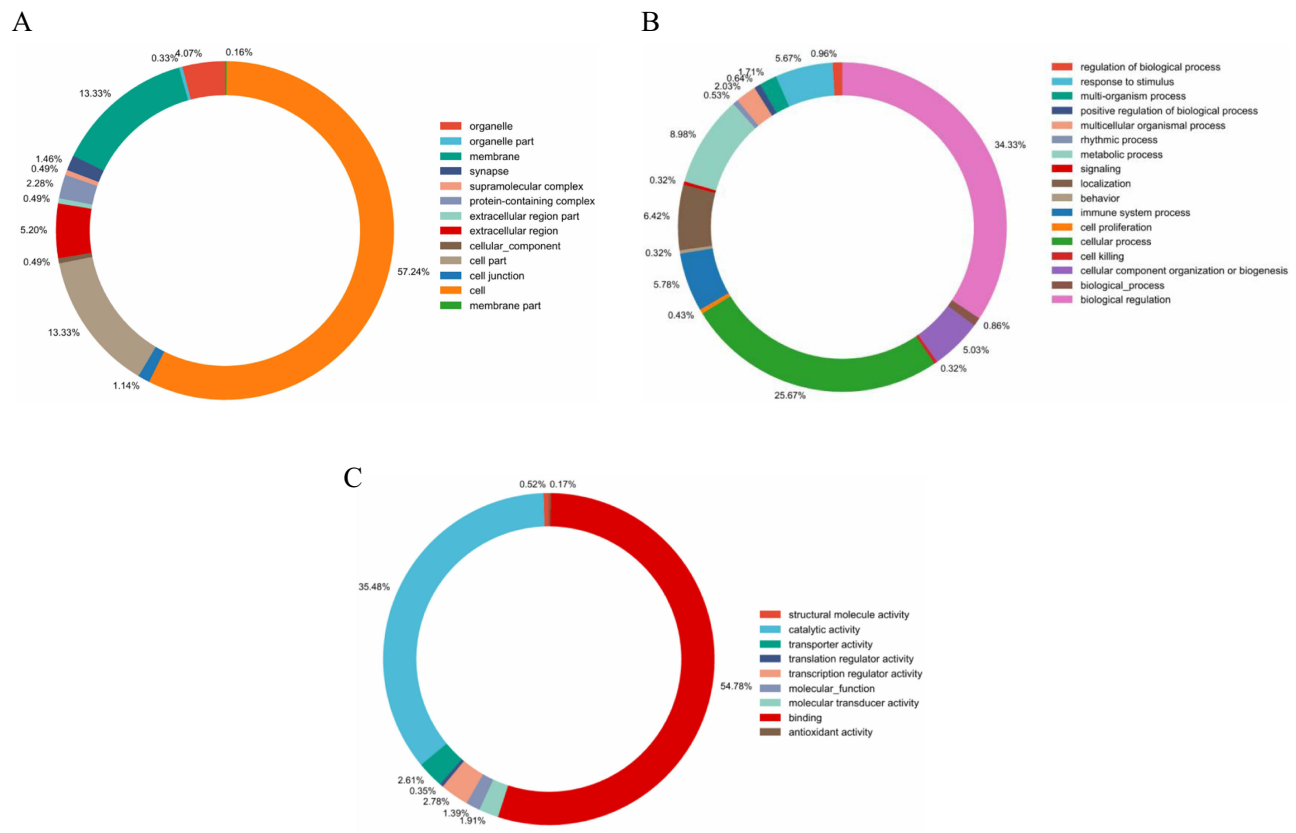

Figure 6 Comparative GO analysis results.
Notes: (**A**) Cellular components. (**B**) Biological processes. (**C**) Molecular functions.
Abbreviation: GO, Gene Ontology.

Selection of Key Proteins

On the basis of the analysis and screening of the differentially enriched proteins, Plin2 and Fdps were identified as shared proteins in our research. The relationships between these two proteins and T2DM were determined via the T2DM Knowledge Portal (https://t2d.hugeamp.org/) (Table 2). Plin2 was positively correlated with FBG, whereas Fdps was negatively correlated with FBG. The r values in Figure 9A and B reflect the strength of this correlation. Compared with those in the Con group, the Plin2 and Fdps levels in the Mod group were significantly different ($p<0.05$). Met and STG decreased Plin2 expression and increased Fdps expression ($p<0.05$, $p<0.01$) (Figure 10A and B).

Discussion

Although STG has been clinically used for the treatment of T2DM, the underlying mechanism has not been fully elucidated. Here, we reported a significant increase in FBG and weight loss in the Mod group, which is typical of T2DM. Moreover, the liver index was significantly greater in the Mod group, which may be significantly associated with insulin resistance in the liver.[25] This is one of the major reasons for the elevated FBG in Mod rats. In addition to elevated blood glucose, blood lipids are more often disturbed in individuals with T2DM. In this study, the levels of TC, TG and LDL-C were significantly elevated. However, STG can lower the FBG, liver index, and TC, TG and LDL-C levels, which may be related to its components, including berberine, atractylenolide III, caffeic acid, hesperetin, and homoisoflavonoids.[26–31] Extensive cellular oedema and steatosis were observed in the livers of the Mod group. The findings of Nawrot M and Soon GST et al revealed similar alterations in the liver.[32,33] Liver lipid accumulation was ameliorated in the STG group. The improvement in the liver lipid index and the HE-stained images of the liver tissue also reflected the alleviation of insulin resistance. However, STG had no significant effect on body weight, which is consistent with the weight-lowering effect of its component berberine.[34]

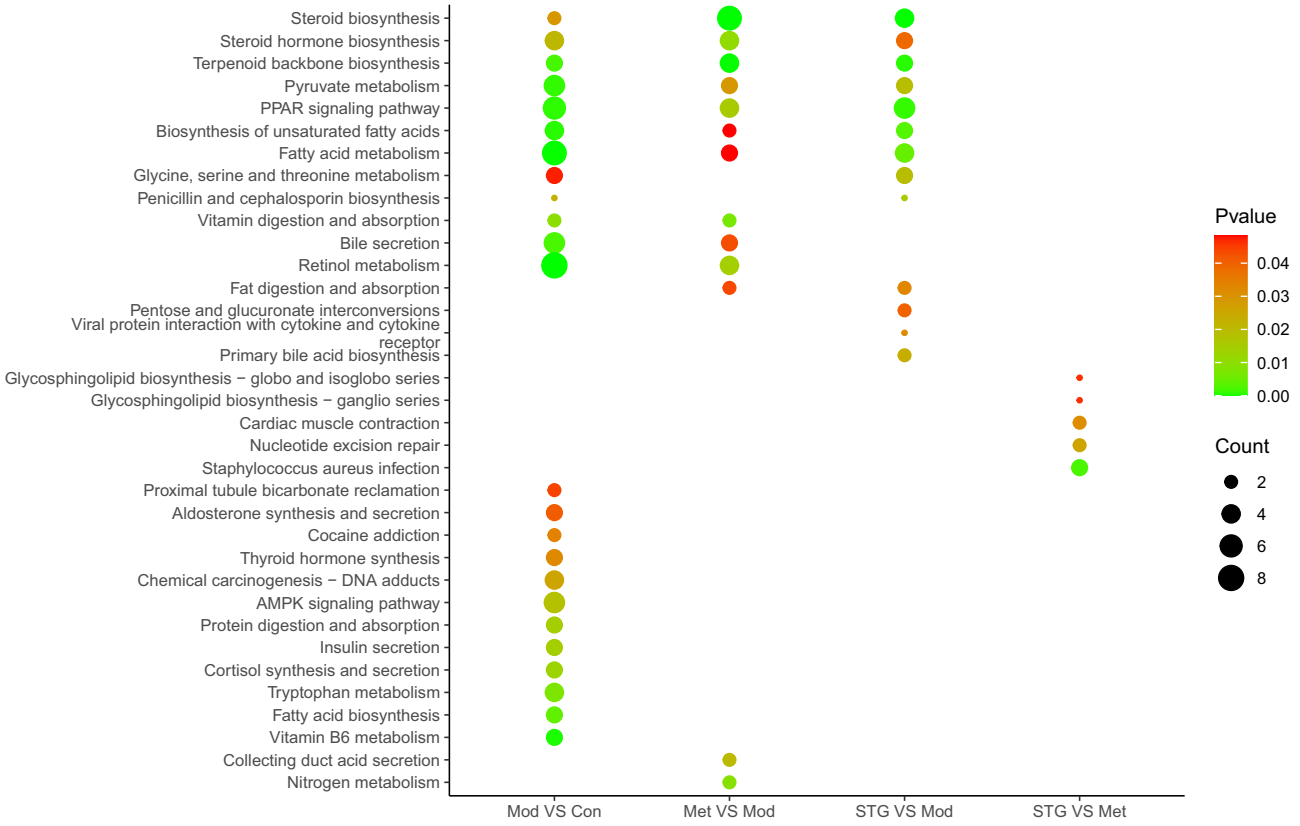

Figure 7 Comparative KEGG pathway analysis.
Abbreviations: Con, control; Mod, model; Met, metformin; STG, Shenzhu Tiaopi granule; KEGG, Kyoto Encyclopedia of Genes and Genomes.

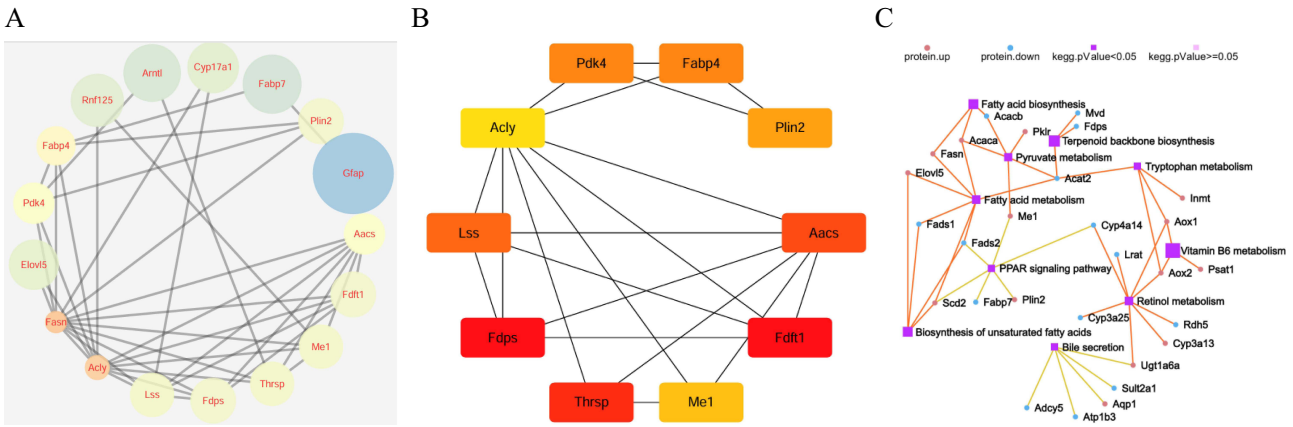

Figure 8 Analysis of target proteins.
Notes: (**A**) Target PPIs. The deeper the yellow colour of the circle is, the smaller its size and the greater its importance. The bluer the colour and the larger the size are, the lesser its importance. (**B**) Core target proteins. The deeper the red colour of the box is, the greater the importance. The yellow colour is less important. (**C**) Network of proteins and KEGG pathways. The purple boxes represent the names of different signalling pathways. The larger the box is, the more significant the difference. The blue dots represent the names of the downregulated proteins. The orange dots represent the names of the upregulated proteins. The orange line represents metabolic pathways, and the yellow line represents organismal system pathways.
Abbreviations: PPI, protein–protein interaction; KEGG, Kyoto Encyclopedia of Genes and Genomes.

In this study, DIA proteomics was used to determine whether STG can regulate proteins in the liver, the target organ of diabetes, to alleviate T2DM. Differentially expressed proteins play important roles in liver cell metabolism. These proteins can participate in intracellular signal transduction via enzyme activity and binding activity, resulting in the regulation of glucose metabolism. In this study, KEGG analysis revealed that insulin secretion, pyruvate metabolism, the

https://doi.org/10.2147/DMSO.S493036

Table 2 Relationships Between Plin2, Fdps and T2DM

Protein	Phenotype	HuGE Score	Evidence Range
Plin2	T2DM adj BMI	3	Moderate
	T2DM	3	Moderate
Fdps	HbA1c	3	Moderate
	Fasting insulin adj BMI	3	Moderate

Abbreviations: T2DM, Type 2 diabetes mellitus; HuGE, Human Genetic Evidence; BMI, body mass index; HbA1c, glycosylated haemoglobin A1c.

PPAR signalling pathway, bile secretion, and the AMPK signalling pathway are related to T2DM. The common pathways of the PPAR signalling pathway and pyruvate metabolism were enriched after STG treatment. This effect may be the main method of intervention. Catalpol is a component of *Codonopsis pilosula* that can normalize insulin sensitivity through the PPAR signalling pathway in mice with T2DM.[35] Fufang Xueshuantong has therapeutic effects on diabetic retinopathy via the PPAR signalling pathway.[36] Hypoxanthine reduces the severity of insulin resistance and decreases FBG via the PPAR signalling pathway.[37] *Agriophyllum* oligosaccharides reduce blood glucose via the PPAR signalling pathway, further protecting the liver in T2DM.[38] *Belamcanda chinensis* (L.) leaves alleviate hyperglycaemia by regulating PPAR to prevent insulin resistance.[39] Berberine, caffeic acid, naringenin, baicalein, atractyloside, hesperetin and ferulic acid are the main components of STG. Berberine, caffeic acid, naringenin and ferulic acid can modulate PPAR expression.[40–43] *Radix Scutellariae*, mulberry leaves and *Coptidis Rhizoma* can regulate pyruvate kinase activity to promote glucose uptake for normalization of glucose metabolism.[44–46] *Coptidis Rhizoma* is also included in STG. Ferulic

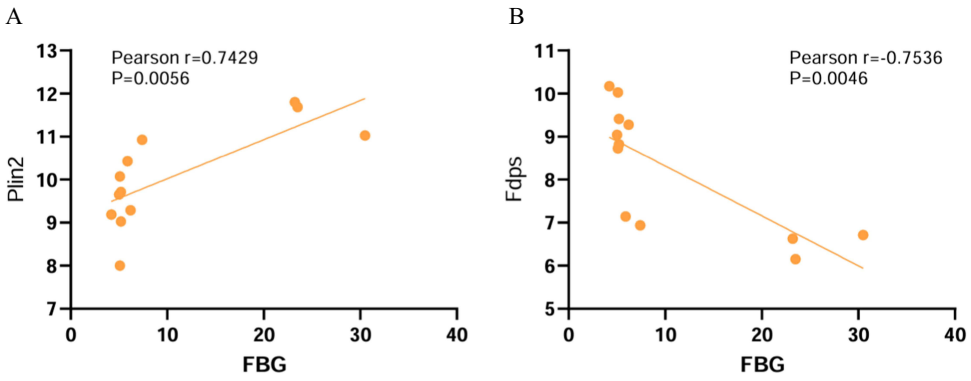

Figure 9 Relationships among Plin2, Fdps and FBG.
Notes: (**A**) Relationships between Plin2 and FBG. (**B**) Relationships between Fdps and FBG.
Abbreviations: FBG, fasting blood glucose.

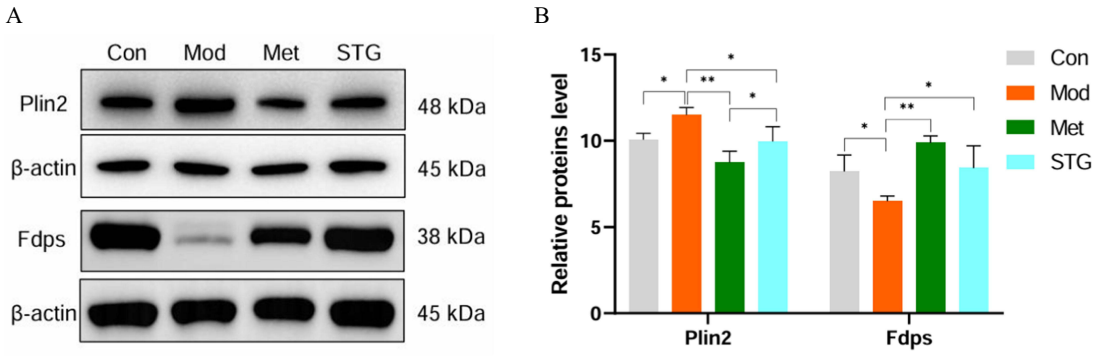

Figure 10 Comparison of the relative levels of Plin2 and Fdps.
Notes: *p<0.05; **p<0.01. (**A**) Plin2 and Fdps expression was evaluated in liver tissue. (**B**) Relative protein ratios of Plin2 and Fdps.
Abbreviations: Con, control; Mod, model; Met, metformin; STG, Shenzhu Tiaopi granule.

acid might be a good supplement to metformin and thiazolidinedione for managing blood glucose.[47] Baicalein, atractyloside, hesperetin and berberine may affect pyruvate activity and inhibit hepatic gluconeogenesis.[44,48–50] Caffeic acid phenethyl ester is a derivative of caffeic acid. This molecule also has a similar role.[51] Most Plin proteins regulate lipolysis, and Plin2 is prone to free fatty acid spillover, which can lead to the induction of apoptosis and insulin resistance in β-cells.[52] Plin2 can ameliorate T2DM by mitigating endoplasmic reticulum stress and restoring β cells.[53,54] Plin2 is commonly expressed in the liver and has been associated with liver insulin sensitivity.[55,56] Plin2 overexpression increases the expression of GSK3, which affects blood glucose levels.[57] In our study, Plin2 expression was upregulated in the Mod group and was found to be positively correlated with FBG. After intervention with STG, FBG decreased, which was related to a decrease in Plin2 expression. In mice intraperitoneally injected with iron dextran, glucose tolerance was significantly reduced.[58] Sphingosine-1 phosphate lyase downregulates Plin2, which regulates pancreatic beta-cell failure in T2DM.[59] Acute exercise in GK rats with T2DM can downregulate Plin2 and normalize blood glucose.[60] Plin2 overexpression leads to inflammatory pathways, thus inhibiting insulin-induced glucose uptake and causing insulin resistance.[61] Loss of Plin2 attenuated FBG and insulin sensitivity.[62] Plin2 is involved in lipid homeostatic regulation. When the sensitivity of the liver and fat to insulin decreases, insulin resistance occurs, which affects the insulin signalling pathway. This process is related to the ability of Plin2 to improve insulin resistance in the liver.[63] Attempts have been made to use PPAR to treat T2DM.[64] Plin2 is involved in the PPAR signalling pathway.[65] These results suggest that Plin2 could be a potential target for further studies.

Fdps plays an important role in various biological processes.[66] For example, Fdps has been implicated in the pathogenesis of diabetic vascular lesions.[67] In our study, Fdps expression was downregulated in the Mod group and was negatively correlated with FBG. After intervention with STG, FBG decreased, which was related to the increase in Fdps expression. Fdps was found to be associated with terpenoid backbone biosynthesis.[68,69] Notably, metformin can regulate terpenoid backbone biosynthesis pathways. In our study, STG also regulated terpenoid backbone biosynthesis.[70] Yu-Ye Tang is widely used to treat T2DM because it regulates terpenoid backbone biosynthesis.[71] These results suggest that Fdps could be a potential target for further studies.

Pdk4 is closely related to glucose metabolism. This molecule may be involved in apoptosis and insulin resistance.[72] Rosiglitazone is a hypoglycaemic drug that can upregulate genes and lower blood glucose.[73] STG also has similar effects. In addition, low Pdk4 expression may induce wound healing in patients with diabetes.[74] Fdft1 is a member of the cholesterol metabolism network and represents a molecular link of T2DM.[75] In this study, Pdk4 has an indirect connection with Fdft1. Fmr1 is a biomarker that participates in the occurrence and progression of diabetic nephropathy.[76] Although this study revealed that STG has an effect on different proteins, the specific mechanism still needs further research in the future.

In conclusion, the present study confirmed that STG can normalize glucose and lipid metabolism in individuals with T2DM. The significantly differentially expressed proteins in the livers of the rats in the four groups were associated mainly with glucose metabolism. Fdps and Plin2 have been identified as key proteins involved in carbohydrate metabolism. The main signalling pathways affected by STG may be the PPAR signalling pathway and terpenoid backbone biosynthesis. Proteomic research has expanded our understanding of T2DM pathogenesis. The findings presented here reveal potential molecular mechanisms for the treatment of T2DM via TCM. The limitations present in this study also require our attention. We chose GK rats as the model of spontaneous T2DM. Whether these results can be found in other models of T2DM is unclear. We will consider choosing other models of T2DM for further research. This study only quantified the protein levels but did not assess post-translational modifications of the protein. In the future, we will conduct joint analysis to help elucidate protein function and regulatory mechanisms. In addition, we selected only 8 rats per group, and increasing the number of rats in the later stage is necessary to increase the reliability of the results. Moreover, we observed this phenomenon only in the liver but not in the pancreas, adipose tissue or other tissues related to T2DM. If Fdps and Plin2 exhibit a common trend in multiple tissues, these research results will be highly important. This study is an animal experiment on the treatment of T2DM with TCM. Further validation in T2DM patients is needed to strengthen the conclusions. If liver samples from T2DM patients and healthy volunteers can be obtained, we will conduct proteomic analyses on the liver tissues. Furthermore, the efficacy of the STG as a complementary or alternative treatment for T2DM should be validated. Proteomics can provide comprehensive protein information, providing new perspectives and methods

for the diagnosis, treatment, and prevention of diseases. TCM has the advantages of multiple targets and multiple pathway interventions in diseases, so this is a good method for using proteomics to identify the molecular targets of TCM. Moreover, we hope that proteomics can be applied to the study of TCM in the treatment of other diseases.

Institutional Review Board Statement

The animal experiments were performed in accordance with the guidelines and approved by the Animal Ethics Committee of Anhui Chinese Medicine University.

Data Sharing Statement

The datasets generated during the current study are available from the iProX. The accession number is IPX0009543000. All the data used in this study are available.

Acknowledgments

The authors extend their appreciation to BGI Shenzhen and Majorbio Bio-Pharm Technology Co., Ltd.

Author Contributions

All authors contributed to data analysis, drafting or revising the article, have agreed on the journal to which the article will be submitted, gave final approval of the version to be published, and agree to be accountable for all aspects of the work.

Funding

The research was funded by the University Scientific Research Projects of Anhui (2023AH050782), open bidding for selecting the best candidates for Xin'an medicine and the modernization of Traditional Chinese Medicine of IHM (2023CXMMTCM024, 2023CXMMTCM003), the Scientific Research Project of Health and Wellness in Anhui Province (AHWJ2023BAc10002), the Anhui Province Outstanding Talents Cultivation Project for Universities (2022-371), Anhui University Collaborative Innovation Project (GXXT-2020-025) and the Anhui Province Health Backbone Talent Training Target (2022-392).

Disclosure

The authors declare that they have no personal, financial, commercial, or conflicts of interest. ARRIVE guidelines statement: The manuscript has been revised according to the ARRIVE guidelines checklist.

References

1. Laffel LM, Danne T, Klingensmith GJ, et al. Efficacy and safety of the SGLT2 inhibitor empagliflozin versus placebo and the DPP-4 inhibitor linagliptin versus placebo in young people with type 2 diabetes (DINAMO): a multicentre, randomised, double-blind, parallel group, Phase 3 trial. *Lancet Diabetes Endocrinol*. 2023;11(3):169–181. doi:10.1016/S2213-8587(22)00387-4
2. Chen Y, Wang M. New insights of anti-hyperglycemic agents and traditional Chinese medicine on gut microbiota in type 2 diabetes. *Drug Des Devel Ther*. 2021;15(12):4849–4863. doi:10.2147/DDDT.S334325
3. Zhang Y, Lee FY, Barrera G, et al. Activation of the nuclear receptor FXR improves hyperglycemia and hyperlipidemia in diabetic mice. *Proc Natl Acad Sci USA*. 2006;103(4):1006–1011. doi:10.1073/pnas.0506982103
4. McGuire DK, Busui RP, Deanfield J, et al. Effects of oral semaglutide on cardiovascular outcomes in individuals with type 2 diabetes and established atherosclerotic cardiovascular disease and/or chronic kidney disease: design and baseline characteristics of SOUL, a randomized trial. *Diabetes Obes Metab*. 2023;25(7):1932–1941. doi:10.1111/dom.15058
5. Christians U, Klawitter J, Klawitter J. Biomarkers in transplantation--proteomics and metabolomics. *Ther Drug Monit*. 2016;38(Suppl 1):S70–S74. doi:10.1097/FTD.0000000000000243
6. Eldjarn GH, Ferkingstad E, Lund SH, et al. Large-scale plasma proteomics comparisons through genetics and disease associations. *Nature*. 2024;630(8015):E3. doi:10.1038/s41586-024-07549-z
7. Collins BC, Hunter CL, Liu Y, et al. Multi-laboratory assessment of reproducibility, qualitative and quantitative performance of SWATH-mass spectrometry. *Nat Commun*. 2017;8(1):291–302. doi:10.1038/s41467-017-00249-5
8. Fu J, Luo Y, Mou M, et al. Advances in current diabetes proteomics: from the perspectives of label- free quantification and biomarker selection. *Curr Drug Targets*. 2020;21(1):34–54. doi:10.2174/1389450120666190821160207
9. Yuan S, Xu F, Li X, et al. Plasma proteins and onset of type 2 diabetes and diabetic complications: proteome-wide Mendelian randomization and colocalization analyses. *Cell Rep Med*. 2023;4(9):101174. doi:10.1016/j.xcrm.2023.101174

10. Nunez Lopez YO, Iliuk A, Petrilli AM, et al. Proteomics and phosphoproteomics of circulating extracellular vesicles provide new insights into diabetes pathobiology. *Int J mol Sci*. 2022;23(10):5779. doi:10.3390/ijms23105779
11. Lao Y, Wang X, Xu N, Zhang H, Xu H. Application of proteomics to determine the mechanism of action of traditional Chinese medicine remedies. *J Ethnopharmacol*. 2014;155(1):1–8. doi:10.1016/j.jep.2014.05.022
12. Wang Y, Javed I, Zhang X, Liu D, Zhang C. Role of differential proteomics in studying pharmacological mechanisms of traditional Chinese medicines. *J Pharm Pharm Sci*. 2019;22(1):424–439. doi:10.18433/jpps30429
13. Shao X, Hu G, Lu Y, et al. Discrimination of traditional Chinese medicine syndromes in type 2 diabetic patients based on metabolomics-proteomics profiles. *Int J Anal Chem*. 2023;2023:5722131. doi:10.1155/2023/5722131
14. Zhang SX, Sun H, Sun WJ, et al. Proteomic study of serum proteins in a type 2 diabetes mellitus rat model by Chinese traditional medicine Tianqi Jiangtang Capsule administration. *J Pharm Biomed Anal*. 2010;53(4):1011–1014. doi:10.1016/j.jpba.2010.06.033
15. Shi L, Wang J, He C, et al. Identifying potential therapeutic targets of mulberry leaf extract for the treatment of type 2 diabetes: a TMT-based quantitative proteomic analysis. *BMC Complement Med Ther*. 2023;23(1):308. doi:10.1186/s12906-023-04140-3
16. Zhao JD, Sun M, Li Y, et al. Characterization of gut microbial and metabolite alterations in faeces of Goto Kakizaki rats using metagenomic and untargeted metabolomic approach. *World J Diabetes*. 2023;14(3):255–270. doi:10.4239/wjd.v14.i3.255
17. Zhao J, Li Y, Sun M, et al. The Chinese herbal formula Shenzhu Tiaopi granule results in metabolic improvement in type 2 diabetic rats by modulating the gut microbiota. *Evid Based Compl Alternat Med*. 2019;2019(6):6976394–6976407. doi:10.1155/2019/6976394
18. Yundong Y, Zhaohui F, Yuanyuan W, et al. Effect of Shenzhu Tiaopi granule on hepatic insulin resistance in diabetic Goto-Kakizakirats via liver kinase B1/adenosine 5'-monophosphate/mammalian target of rapamycin signaling pathway. *J Traditional Chin Med*. 2021;41(1):107–116. doi:10.19852/j.cnki.jtcm.2021.01.013
19. Fang Z, Zhao J, Shi G, et al. Shenzhu Tiaopi granule combined with lifestyle intervention therapy for impaired glucose tolerance: a randomized controlled trial. *Complement Ther Med*. 2014;22(5):842–850. doi:10.1016/j.ctim.2014.08.004
20. Zhao J, Fang Z. Alterations of the gut microbiota and metabolites by ShenZhu TiaoPi granule alleviates hyperglycemia in GK rats. *Front Microbiol*. 2024;15:1420103. doi:10.3389/fmicb.2024.1420103
21. Wang J, Liang Q, Zhao Q, et al. The effect of microbial composition and proteomic on improvement of functional constipation by Chrysanthemum morifolium polysaccharide. *Food Chem Toxicol*. 2021;153:112305. doi:10.1016/j.fct.2021.112305
22. Yan K, Bai B, Ren Y, et al. The comparable microenvironment shared by colorectal adenoma and carcinoma: an evidence of stromal proteomics. *Front Oncol*. 2022;12:848782. doi:10.3389/fonc.2022.848782
23. Han B, Jian Y, Xia X, et al. Studying the effects of sea cucumber ovum powder on nonalcoholic fatty liver disease by proteomics techniques in a rat model. *Food Funct*. 2020;11(7):6139–6147. doi:10.1039/D0FO00741B
24. Choi M, Chang CY, Clough T, et al. MSstats: an R package for statistical analysis of quantitative mass spectrometry-based proteomic experiments. *Bioinformatics*. 2014;30(17):2524–2526. doi:10.1093/bioinformatics/btu305
25. Jung CH, Lee WJ, Hwang JY, et al. Assessment of the fatty liver index as an indicator of hepatic steatosis for predicting incident diabetes independently of insulin resistance in a Korean population. *Diabet Med*. 2013;30(4):428–435. doi:10.1111/dme.12104
26. Kong W, Li Z, Xiao X, et al. Quality control for Coptidis rhizoma through the determination of five alkaloids by HPLC–ELSD coupled with chemometrics. *Nat Prod Res*. 2010;24(17):1616–1629. doi:10.1080/14786411003757937
27. Song MY, Jung HW, Kang SY, Park YK. Atractylenolide III enhances energy metabolism by increasing the SIRT-1 and PGC1α expression with AMPK phosphorylation in C2C12 mouse skeletal muscle cells. *Biol Pharm Bull*. 2017;40(3):339–344. doi:10.1248/bpb.b16-00853
28. Jia W, Bi Q, Jiang S, et al. Hypoglycemic activity of Codonopsis pilosula (Franch.) Nannf. in vitro and in vivo and its chemical composition identification by UPLC-Triple-TOF-MS/MS. *Food Funct*. 2022;13(5):2456–2464. doi:10.1039/D1FO03761G
29. Oršolić N, Sirovina D, Odeh D, et al. Efficacy of caffeic acid on diabetes and its complications in the mouse. *Molecules*. 2021;26(11):3262. doi:10.3390/molecules26113262
30. Yang H, Wang Y, Xu S, et al. Hesperetin, a promising treatment option for diabetes and related complications: a literature review. *J Agric Food Chem*. 2022;70(28):8582–8592. doi:10.1021/acs.jafc.2c03257
31. Wang Y, Liu F, Liang Z, et al. Homoisoflavonoids and the antioxidant activity of Ophiopogon *japonicus* root. *Iran J Pharm Res*. 2017;16 (1):357–365.
32. Nawrot M, Peschard S, Lestavel S, et al. Intestine-liver crosstalk in type 2 diabetes and non-alcoholic fatty liver disease. *Metabolism*. 2021;123 (8):154844–154892. doi:10.1016/j.metabol.2021.154844
33. Soon GST, Torbenson M. The liver and glycogen: in sickness and in health. *Int J mol Sci*. 2023;24(7):6133–6146. doi:10.3390/ijms24076133
34. Gasmi A, Asghar F, Zafar S, et al. Berberine: pharmacological features in health disease and aging. *Curr Med Chem*. 2024;31(10):1214–1234. doi:10.2174/0929867330666230207112539
35. Yap KH, Yee GS, Candasamy M, et al. Catalpol ameliorates insulin sensitivity and mitochondrial respiration in skeletal muscle of type-2 diabetic mice through insulin signaling pathway and AMPK/SIRT1/PGC-1α/PPAR-γ activation. *Biomolecules*. 2020;10(10):1360. doi:10.3390/biom10101360
36. Sun HH, Chai XL, Li HL, et al. Fufang Xueshuantong alleviates diabetic retinopathy by activating the PPAR signalling pathway and complement and coagulation cascades. *J Ethnopharmacol*. 2021;265:113324. doi:10.1016/j.jep.2020.113324
37. Huang S, Liang H, Chen Y, et al. Hypoxanthine ameliorates diet-induced insulin resistance by improving hepatic lipid metabolism and gluconeogenesis via AMPK/mTOR/PPARα pathway. *Life Sci*. 2024;357:123096. doi:10.1016/j.lfs.2024.123096
38. Bao S, Wu YL, Wang X, et al. Agriophyllum oligosaccharides ameliorate hepatic injury in type 2 diabetic db/db mice targeting INS-R/IRS-2/PI3K/AKT/PPAR-γ/Glut4 signal pathway. *J Ethnopharmacol*. 2020;257:112863. doi:10.1016/j.jep.2020.112863
39. Guo Y, Dai R, Deng Y, Sun L, Meng S, Xin N. Hypoglycemic activity of the extracts of Belamcanda chinensis leaves (BCLE) on KK-A^y mice. *Biomed Pharmacother*. 2019;110:449–455. doi:10.1016/j.biopha.2018.11.094
40. Zhou J, Zhou S. Berberine regulates peroxisome proliferator-activated receptors and positive transcription elongation factor b expression in diabetic adipocytes. *Eur J Pharmacol*. 2010;649(1–3):390–397. doi:10.1016/j.ejphar.2010.09.030
41. Vasileva LV, Savova MS, Amirova KM, et al. Caffeic and chlorogenic acids synergistically activate browning program in human adipocytes: implications of AMPK- and PPAR-mediated pathways. *Int J mol Sci*. 2020;21(24):9740. doi:10.3390/ijms21249740

42. Qi Z, Xu Y, Liang Z, et al. Naringin ameliorates cognitive deficits via oxidative stress, proinflammatory factors and the PPARγ signaling pathway in a type 2 diabetic rat model. *Mol Med Rep*. 2015;12(5):7093–7101. doi:10.3892/mmr.2015.4232
43. Jung CH, Lee DH, Ahn J, et al. γ-oryzanol enhances adipocyte differentiation and glucose uptake. *Nutrients*. 2015;7(6):4851–4861. doi:10.3390/nu7064851
44. Yang Z, Huang W, Zhang J, Xie M, Wang X. Baicalein improves glucose metabolism in insulin resistant HepG2 cells. *Eur J Pharmacol*. 2019;854:187–193. doi:10.1016/j.ejphar.2019.04.005
45. Li JS, Ji T, Su SL, et al. Mulberry leaves ameliorate diabetes via regulating metabolic profiling and AGEs/RAGE and p38 MAPK/NF-κB pathway. *J Ethnopharmacol*. 2022;283:114713. doi:10.1016/j.jep.2021.114713
46. Cui X, Qian DW, Jiang S, Shang EX, Zhu ZH, Duan JA. Scutellariae radix and coptidis rhizoma improve glucose and lipid metabolism in T2DM rats via regulation of the metabolic profiling and MAPK/PI3K/Akt signaling pathway. *Int J mol Sci*. 2018;19(11):3634. doi:10.3390/ijms19113634
47. Prabhakar PK, Prasad R, Ali S, et al. Synergistic interaction of ferulic acid with commercial hypoglycemic drugs in streptozotocin induced diabetic rats. *Phytomedicine*. 2013;20(6):488–494. doi:10.1016/j.phymed.2012.12.004
48. Siess EA, Wieland OH. Phosphorylation state of cytosolic and mitochondrial adenine nucleotides and of pyruvate dehydrogenase in isolated rat liver cells. *Biochem J*. 1976;156(1):91–102. doi:10.1042/bj1560091
49. Zareei S, Boojar MMA, Amanlou M. Inhibition of liver alanine aminotransferase and aspartate aminotransferase by hesperidin and its aglycone hesperetin: an in vitro and in silico study. *Life Sci*. 2017;178:49–55. doi:10.1016/j.lfs.2017.04.001
50. Gupta M, Rumman M, Singh B, Mahdi AA, Pandey S. Berberine ameliorates glucocorticoid-induced hyperglycemia: an in vitro and in vivo study. *Naunyn Schmiedebergs Arch Pharmacol*. 2024;397(3):1647–1658. doi:10.1007/s00210-023-02703-2
51. Celik S, Erdogan S, Tuzcu M. Caffeic acid phenethyl ester (CAPE) exhibits significant potential as an antidiabetic and liver-protective agent in streptozotocin-induced diabetic rats. *Pharmacol Res*. 2009;60(4):270–276. doi:10.1016/j.phrs.2009.03.017
52. Olofsson SO, Bostrom P, Andersson L, et al. Lipid droplets and their role in the development of insulin resistance and diabetic dyslipidemia. *Clin Lipidol*. 2009;4(5):611-622. doi:10.2217/clp.09.54
53. Chen E, Tsai TH, Li L, Saha P, Chan L, Chang BH. PLIN2 is a key regulator of the unfolded protein response and endoplasmic reticulum stress resolution in pancreatic β cells. *Sci Rep*. 2017;7(1):40855. doi:10.1038/srep40855
54. Ji J, Petropavlovskaia M, Khatchadourian A, et al. Type 2 diabetes is associated with suppression of autophagy and lipid accumulation in β-cells. *J Cell Mol Med*. 2019;23(4):2890–2900. doi:10.1111/jcmm.14172
55. Sentinelli F, Capoccia D, Incani M, et al. The perilipin 2 (PLIN2) gene Ser251Pro missense mutation is associated with reduced insulin secretion and increased insulin sensitivity in Italian obese subjects. *Diabetes Metab Res Rev*. 2016;32(6):550–556. doi:10.1002/dmrr.2751
56. Conte M, Franceschi C, Sandri M, et al. Perilipin 2 and age-related metabolic diseases: a new perspective. *Trends Endocrinol Metab*. 2016;27(12):893–903. doi:10.1016/j.tem.2016.09.001
57. Liu X, Lu X, Song K, Blackman MR. Natural functions of PLIN2 mediating Wnt/LiCl signaling and glycogen synthase kinase 3 (GSK3)/GSK3 substrate-related effects are modulated by lipid. *mol Cell Biol*. 2015;36(3):421–437. doi:10.1128/MCB.00510-15
58. Ma W, Jia L, Xiong Q, et al. Iron overload protects from obesity by ferroptosis. *Foods*. 2021;10(8):1787. doi:10.3390/foods10081787
59. Tang Y, Plötz T, Gräler MH, Gurgul-Convey E. Sphingosine-1 phosphate lyase regulates sensitivity of pancreatic beta-cells to lipotoxicity. *Int J mol Sci*. 2021;22(19):10893. doi:10.3390/ijms221910893
60. Fu S, Meng Y, Lin S, et al. Transcriptomic responses of hypothalamus to acute exercise in type 2 diabetic Goto-Kakizaki rats. *PeerJ*. 2019;7:e7743. doi:10.7717/peerj.7743
61. Cho KA, Kang PB. PLIN2 inhibits insulin-induced glucose uptake in myoblasts through the activation of the NLRP3 inflammasome. *Int J Mol Med*. 2015;36(3):839–844. doi:10.3892/ijmm.2015.2276
62. Chang BH, Li L, Saha P, Chan L. Absence of adipose differentiation related protein upregulates hepatic VLDL secretion, relieves hepatosteatosis, and improves whole body insulin resistance in leptin-deficient mice. *J Lipid Res*. 2010;51(8):2132–2142. doi:10.1194/jlr.M004515
63. Okada-Iwabu M, Yamauchi T, Iwabu M, et al. A small-molecule AdipoR agonist for type 2 diabetes and short life in obesity. *Nature*. 2013;503(7477):493–499. doi:10.1038/nature12656
64. Maréchal L, Laviolette M, Rodrigue-Way A, et al. The CD36-PPARγ Pathway in Metabolic Disorders. *Int J mol Sci*. 2018;19(5):1529. doi:10.3390/ijms19051529
65. Dai ZW, Cai KD, Xu LC, Wang LL. Perilipin2 inhibits diabetic nephropathy-induced podocyte apoptosis by activating the PPARγ signaling pathway. *mol Cell Probes*. 2020;53(10):101584. doi:10.1016/j.mcp.2020.101584
66. Liu X, Liu Y, Tang L, et al. Inhibition of farnesyl pyrophosphate synthase alleviates cardiomyopathy in diabetic rat. *Cell Cycle*. 2023;22(6):666–679. doi:10.1080/15384101.2022.2139126
67. Liu XW, Jin HF, Du CQ, et al. Farnesyl pyrophosphate synthase blocker ibandronate reduces thoracic aortic fibrosis in diabetic rats. *Am J Med Sci*. 2019;357(4):323–332. doi:10.1016/j.amjms.2019.01.014
68. Hassani SF, Sayaf M, Danandeh SS, et al. Novel insight into the association between obesity and hepatocellular carcinoma occurrence and recurrence: high-throughput microarray data set analysis of differentially expressed genes. *JCO Clin Cancer Inform*. 2021;5(5):1169–1180. doi:10.1200/CCI.21.00094
69. Si Y, Wen H, Li Y, et al. Liver transcriptome analysis reveals extensive transcriptional plasticity during acclimation to low salinity in Cynoglossus semilaevis. *BMC Genomics*. 2018;19(1):464. doi:10.1186/s12864-018-4825-4
70. Lake J, Bortolasci CC, Stuart AL, et al. Metformin is protective against the development of mood disorders. *Pharmacopsychiatry*. 2023;56(1):25–31. doi:10.1055/a-1936-3580
71. Ma Z, Sun W, Wang L, et al. Integrated 16S rRNA sequencing and nontargeted metabolomics analysis to reveal the mechanisms of Yu-Ye Tang on type 2 diabetes mellitus rats. *Front Endocrinol*. 2023;14:1159707. doi:10.3389/fendo.2023.1159707
72. Dlamini Z, Ntlabati P, Mbita Z, et al. Pyruvate dehydrogenase kinase 4 (PDK4) could be involved in a regulatory role in apoptosis and a link between apoptosis and insulin resistance. *Exp Mol Pathol*. 2015;98(3):574–584. doi:10.1016/j.yexmp.2015.03.022
73. Wei P, Lin D, Luo C, et al. High glucose promotes benign prostatic hyperplasia by downregulating PDK4 expression. *Sci Rep*. 2023;13(1):17910. doi:10.1038/s41598-023-44954-2
74. Ma Z, Mo R, Yang P, et al. PDK4 facilitates fibroblast functions and diabetic wound healing through regulation of HIF-1α protein stability and gene expression. *FASEB J*. 2023;37(10):e23215. doi:10.1096/fj.202300874RR

75. Ding J, Reynolds LM, Zeller T, et al. Alterations of a cellular cholesterol metabolism network are a molecular feature of obesity-related type 2 diabetes and cardiovascular disease. *Diabetes*. 2015;64(10):3464–3474. doi:10.2337/db14-1314
76. Hu K, He R, Xu M, et al. Identification of necroptosis-related features in diabetic nephropathy and analysis of their immune microenvironent and inflammatory response. *Front Cell Dev Biol*. 2023;11:1271145. doi:10.3389/fcell.2023.1271145

Diabetes, Metabolic Syndrome and Obesity

Dovepress
Taylor & Francis Group

Publish your work in this journal

Diabetes, Metabolic Syndrome and Obesity is an international, peer-reviewed open-access journal committed to the rapid publication of the latest laboratory and clinical findings in the fields of diabetes, metabolic syndrome and obesity research. Original research, review, case reports, hypothesis formation, expert opinion and commentaries are all considered for publication. The manuscript management system is completely online and includes a very quick and fair peer-review system, which is all easy to use. Visit http://www.dovepress.com/testimonials.php to read real quotes from published authors.

Submit your manuscript here: https://www.dovepress.com/diabetes-metabolic-syndrome-and-obesity-journal